Biological clock in total darkness: The *Clock*/*MOP3* circadian system of the blind subterranean mole rat

Aaron Avivi*, Urs Albrecht†, Henrik Oster†, Alma Joel*, Avigdor Beiles*, and Eviatar Nevo*‡

*Institute of Evolution, University of Haifa, Mount Carmel, Haifa 31905, Israel; and †Max Planck Institute for Experimental Endocrinology, 30625 Hannover, Germany

Contributed by Eviatar Nevo, September 20, 2001

Blind subterranean mole rats retain a degenerated, subcutaneous, visually blind but functionally circadian eye involved in photoperiodic perception. Here we describe the cloning, sequence, and expression of the circadian *Clock* and *MOP3* cDNAs of the *Spalax ehrenbergi* superspecies in Israel. Both genes are relatively conserved, although characterized by a significant number of amino acid substitutions. The glutamine-rich area of Clock, which is assumed to function in circadian rhythmicity, is expanded in *Spalax* compared with that of humans and mice, and is different in amino acid composition from that of rats. We also show that MOP3 is a bona fide partner of *Spalax* Clock and that the *Spalax* Clock/MOP3 dimer is less potent than its human counterpart in driving transcription. We suggest that this reduction in transcriptional activity may be attributed to the *Spalax* Clock glutamine-rich domain, which is unique in its amino acid composition compared with other studied mammalian species. Understanding *Clock*/*MOP3* function could highlight circadian mechanisms in blind mammals and their unique pattern as a result of adapting to life underground.

Biological Clocks Underground

The behavior of all eukaryotic organisms is characterized by a 24-h cycle of rest and activity, as a fundamental adaptation to the solar cycle of light and darkness (1–4). In mammals, the pacemaker of this circadian rhythm is localized in the central nervous system (5) and it is entrained by light signals in the eye. An intriguing question is how a subterranean, naturally blind mammal with a subcutaneous degenerated eye maintains its circadian system, and whether its examination can illuminate circadian rhythmicity of sighted mammals above ground.

The underground adaptive ecogeographical radiation of the *Spalax ehrenbergi* superspecies in Israel involves four sibling species: *Spalax galili*, *Spalax golani*, *Spalax carmeli*, and *Spalax judaei*, with diploid chromosome numbers $2n = 52$, 54, 58, and 60, respectively (6), displaying progressive stages of final ecological speciation (7, 8). Their adaptive radiation in Israel, from early Pleistocene to Recent times, is closely associated with increasing aridity stress, hence, with distinct climatic diversity. *S. galili*, radiated in the cool-humid northern upper Galilee Mountains; *S. golani*, in the cool-semidry northeastern Golan Heights; *S. carmeli*, in warm-humid central Israel; and *S. judaei*, in warm-dry southern Samaria, Judea, and the northern Negev mountains and plains.

Spalax represents an extreme example of natural eye and brain reorganization in mammals (8, 9). The animal is completely blind (10), yet the retina of the atrophied subcutaneous eye functions in photoentrainment of locomotor activity and thermoregulatory rhythms (11–13). Ocular regression of thalamic sight structures conceals adaptive progression of the photoperiodic system (14, 15). Retinal rhodopsin (16) and coneopsin participate in photoentrainment (17, 18). *Per*-homologous ACNGGN sequence comprising poly(Thr-Gly) shows hypothalamic circadian oscillation (19). Thus, *Spalax* displays behavioral circadian rhythm adapted to life underground.

Activity patterns were tested in the four sibling species of the *S. ehrenbergi* superspecies (20). Activity patterns were found to be polyphasic and polymorphic (19, 20), with a remarkable intra- and interspecies diversity in circadian patterns (refs. 21 and 22—no species is identified in the latter study) coupled with seasonal shifts.[§] This complex pattern is unique in mammals analyzed to date. These patterns may display an adaptive strategy of a subterranean mammal, safeguarded from above-ground predation.

Molecular Genetic Basis of Circadian Rhythms

In recent years, tremendous progress has been achieved in revealing the molecular-genetic basis of circadian activity in different organisms across phylogeny, including cyanobacteria, plants, fungi, insects, and mammals (1, 23). All show homologous circadian molecules, both structurally and functionally (23). The circadian genes identified in mammals are *Clock*, *MOP3*, *Per1*, *Per2*, *Per3*, *Tim*, *Cry1*, and *Cry2* (23), all interacting in circadian rhythmicity. In *Drosophila*, the sex-linked period (*Per*) gene affects rhythmicity in circadian (24-h), ultradian (<24-h), and infradian (>24-h) time domains (24). Work in *Drosophila* and mice suggested a mechanism in which expression of *Per* genes is driven by a CLOCK/MOP3 heterodimer, which, through their basic helix–loop–helix (bHLH) motif and the PAS domains, binds to the E-box present in the *Per* promoter, thereby activating *Per* transcription. PER/TIM and PER/CRY complexes probably block the activation of *Per* transcription by interfering with the activity of Clock/MOP3 (25). Indeed, it was recently proven (26) that the loss of PAS protein MOP3 in mice results in immediate and complete loss of circadian rhythmicity. Recent studies (27) more specifically clarify the detailed mechanism of the regulation of the circadian rhythm. Studying mutant *Clock*, *Per2*, and *Cry* of mice, Shearman *et al.* (27) showed that *Per2* has a dominant role in the positive regulation of the *MOP3,* whereas the *Crys* are the negative regulators of the *Per* and *Cry* cycles. *Clock* mutants appear to positively alter the regulation of *MOP3* gene expression in the suprachiasmatic nucleus (SCN), but not the regulation of *Clock* itself. As the oscillations of the *Pers* and *Crys* RNA are down-regulated in the *Clock* mutant mice, the effect of Clock on MOP3 levels is probably indirect and may occur through the Pers and/or the Crys proteins; the reduced levels of one or more of these genes may cause the reduced levels of *MOP3* in the *Clock* mutant mice through loss of the positive control of *MOP3* transcription.

The underlying genetic basis of circadian rhythms in the blind, subterranean mole rats may be different from that of strictly diurnal or nocturnal and sighted mammals, such as humans and mice, which presumably lack multiphasic, polymorphic, and

EVOLUTION

Abbreviations: RT, reverse transcriptase; bHLH, basic helix–loop–helix; SCN, suprachiasmatic nucleus; RLU, relative light unit; polyQ, polyglutamine; h*Clock*, human *Clock*; s*Clock*, *Spalax Clock*.

Data deposition: The sequences reported in this paper have been deposited in the GenBank database (accession nos. AJ318057–AJ318060).

‡To whom reprint requests should be addressed. E-mail: nevo@research.haifa.ac.il.

§Kushnirov, D., Beolchini, F., Lombardini, F. & Nevo, E. (1998) Euro-American Mammal Congress, July 19–24, 1998, Santiago de Compostela, Spain, abstr. 381.

The publication costs of this article were defrayed in part by page charge payment. This article must therefore be hereby marked "*advertisement*" in accordance with 18 U.S.C. §1734 solely to indicate this fact.

seasonal biological circadian patterns. The coupled ecological and phylogenetic uniqueness of *Spalax* makes it an intriguing model organism for assessing the molecular-genetic machinery of the biological clock.

Our objectives in this study were to compare and contrast the structure and the expression of the *Clock* gene in the blind subterranean mole rat with those of other mammals, and suggest experiments for its potential effects on the unique circadian rhythmicity of these species. We show differences in *Clock* structure and expression between mole rats, rats, mice, and humans. We also demonstrate differences among three mole rat species whose significance may derive from the ecological differences of the species—a testable hypothesis.

Materials and Methods

Animals. Animals used for the cloning of the mole rat *Clock* belong to three species of the *S. ehrenbergi* superspecies in Israel (6–8). The species name is followed by the diploid chromosome number, population name, and the geographic region: *S. galili,* $2n = 52$, Kerem Ben Zimra, Upper Galilee; *S. carmeli*, $2n = 58$, Muhraka, Mt. Carmel; *S. judaei*, $2n = 60$, Anza, Samaria. The *S. galili* was also used for the cloning of *MOP3*. All of the animals used in these experiments were captured in the field and kept in our animal facility for at least 3 months before use. Animals were housed in individual cages, each species in a separate room. They were kept under controlled conditions of 22–24°C with seasonal light/dark hours and fed with carrots and apples. Animals used in this study were adults and of similar weight (100–150 g).

Cloning. By reverse transcriptase (RT)-PCR (28), we cloned the complete ORF of *Clock* from three individuals each belonging to a different species as described above. The oligonucleotides used for the RT-PCR cloning were designed according to the published sequence of human *Clock* (GenBank accession no. AF011568) and that of the mouse (GenBank accession no. AF000998). These were a 5′ sense oligonucleotide 5′-ACAAGACGAAAAC(GA)TA-(GA)T(AG)TGTTATG (the 3′ ATG is the initiation codon), and a 3′ antisense oligonucleotide 5′-AGAGAGGAAG(CT)(AG)-(CT)GTGTGCTA (the 3′ CTA is the termination codon).

To construct the *S. galili Clock* cDNA with a replaced human Q-rich (glutamine-rich) domain (s*Clock*-hQ) and the human equivalent (h*Clock*-sQ), *Clock* cDNA fragments from both species, equivalent to *Spalax* amino acids numbers 1–744 and 736–865 (see GenBank accession no. AJ318057) were amplified and joined by PCR.

Spalax MOP3 cDNA was also cloned by RT-PCR from *S. galili* brain tissue by using oligonucleotides designed according to the published sequence of human *MOP3* (GenBank accession no. AF044288) and that of the mouse (GenBank accession no. AB015203). These were a 5′ sense oligonucleotide 5′-TG(T/C)(G/A)A(C/G)(T/C)(T/A)C(A/C)G(A/T)(T/C)C(A/T)TCCAATG (the 3′ ATG is the initiation codon) and a 3′ antisense oligonucleotide 5′GCCAAAGCAACATGTAGTGT(T/C)(T/C)A. The (T/C)(T/C)A is a combination of the three possible termination codons. The tissues used in this study for the RT-PCR experiments were collected at the same time from all individuals.

Similarity Tree. The tree presented is a protein (amino acids)-based tree using Kimura's protein distance (29). The tree is derived by using the Wisconsin package version 10 (Genetics Computer Group, Madison, WI), using the neighbor-joining method. We chose this method after Weir (30), who summarized the simulation studies and showed that this method is among the best methods based on distance matrices.

Transcriptional Activity. The entire ORFs of *Spalax* (s) and human (h) *Clock* as well as s*Clock*-hQ and h*Clock*-sQ were cloned into the pTARGET expression vector (Promega). Plasmids expressing these constructs were cotransfected with an h*MOP3* or s*MOP3*-expressing plasmid and the M34RE-luciferase reporter plasmid into the human hepatoma cell line Hep3b. The M34RE-luciferase has three E-box elements (the CACGTG sequence), a transcription factor-binding site found in the *Per1* promoter region, in tandem upstream of the luciferase gene (25). Transfections were performed by means of Lipofectamine (Life Technologies). In all experiments, the luciferase reporter activity was normalized to β-galactosidase expression resulting from cotransfection of a control plasmid [a cytomegalovirus (CMV) promoter that drives the expression of the β-galactosidase gene]. Cells were incubated for 20 h before harvest. The luciferase activity was determined as described (25). The relative light units (RLUs) were calculated from the luciferase activity divided by the β-galactosidase activity for each assay.

***In Situ* Hybridization.** Animals used for testing the brains were kept in a controlled environment of 12-h light/12-h dark. All specimens came from diurnal animals, as was proven by monitoring their locomotor activity. *Spalax* brains were removed under sterile conditions at Zeitgeber times ZT0, ZT6, ZT12, and ZT18 (ZT0 is when lights are turned on, and ZT12 is when lights are turned off) and fixed in ice-cold 4% paraformaldehyde/PBS for 16–20 h. Tissues were dehydrated, embedded in paraffin, and sectioned at a thickness of 10 μm. *In situ* hybridization was performed as described (31). The *Clock* probes corresponded to nucleotides 423-1290 of *Spalax* cDNA (amino acids 141–430 in accession no. AJ318057) and the *MOP3* probes to nucleotides 1–864 of *Spalax* cDNA (amino acids 1–288 in accession no. AJ318060). Antisense and sense riboprobes were synthesized with T3 or T7 RNA polymerase in the presence of 5′-α^{35}S-UTP (1,250 Ci/mmol; 1 Ci = 37 GBq; DuPont/NEN). Hybridization was done overnight at 55°C. Stringency washes were performed at 64°C. Slides were dipped in NTP-2 emulsion and exposed for 6 days. Tissue was visualized by fluorescence of Hoechst dye 33258-stained nuclei (blue color in figure). Silver grains were visualized by dark-field illumination. Image is a videograph captured with ADOBE PHOTOSHOP. Experiments were performed in duplicate.

Results

***Spalax Clock* and *MOP3* cDNA Structure.** A full length *Spalax* cDNA for *Clock* was isolated from three of the Israeli species, namely *S. galili*, *S. carmeli*, and *S. judaei*. A full-length cDNA of *Spalax MOP3* was isolated from *S. galili.* The clones were obtained by RT-PCR of brain tissue by using oligonucleotides from the translational initiation and termination sites of the previously published human and mouse counterparts.

The *Spalax Clock* cDNA is over 90% similar to the genes of mice, rats (accession no. NM021856), and humans (for the complete cDNA sequences and the deduced amino acids of the three *Spalax* species see accession nos. AJ318057, AJ318058, and AJ318059). Translated, however, *Spalax Clock* cDNA encodes a protein of 865 aa compared with 855 in mice, 846 in humans, and 862 in rats (32). The Gly-Met-Asn-Thr at positions 610–613 in human, missing in mouse, occur in the three *Spalax* species, though Thr is replaced by Ala in all *Spalax* species. Glutamine at position 629 in mice is missing in humans, and occurs in all *Spalax* species. Table 1 summarizes the synonymous and nonsynonymous mutations among the three *Spalax* species studied and then between them and humans and mice. *Spalax* has 18–26 amino acid substitutions compared with humans, and 35–42 substitutions compared with mice. *S. judaei* (S60) and *S. carmeli* (S58), geographically adjacent species, differ in 8 amino acids and 12 mutations. *S. judaei* differs from the more northern species, *S. galili* (S52), in 10 amino acids and in a total of 13 mutations. *S. galili* and *S. carmeli*, which are geographical neighbors, differ in 3 amino acids and 7 mutations. The bHLH domain and the two PAS domains of *Clock* cDNA are similar in

Table 1. Summary of mutations in *Clock* cDNA

	S52	S58	S60	Mus	Hu
S52	—				
S58	3ns + 4s (7)	—			
S60	10ns + 3s (13)	8ns + 4s (12)	—		
Mus	37ns + 148s (185)	35ns + 150s (185)	42ns + 151s (193)	—	
Hu	18ns + 154s (172)	26ns + 147s (173)	26ns + 152s (178)	25ns + 193s (218)	—

The distances in *Clock* cDNA sequence among the three *Spalax* species studied (S52, S58, and S60), mouse (Mus), and humans (Hu). The distance is expressed in number of synonymous (s) and nonsynonymous (ns) substitutions. The total number of substitutions appears in parentheses. Note the larger number of substitutions between *Spalax* and humans than that between *Spalax* and mouse. Also noteworthy is the unusual larger number of nonsynonymous mutations compared with the synonymous substitutions among the *Spalax* species, indicating interspecies functional changes.

all studied species. The most impressive difference between *Spalax* and humans and mice is in the Q-rich domain as can be seen in Fig. 1. The *Spalax* repeat is 18 aa longer than that found in humans and 5 aa longer than that of mice and it is different in amino acid composition from rats.

The *S. galili MOP3* cDNA (accession no. AJ318060) is also very similar to those of mouse and human. The putative peptide encodes 626 amino acids. Like human *MOP3* (accession no. AF044288), it misses the Leu-Asp-Asp-Phe-Ala-Phe-Glu, which appears in the mouse (position 48 to 54 in the mouse peptide, accession no. AB015203). There are 8 unique amino acid substitutions in the *Spalax* peptide (positions 304, 306, 330, 332, 334, 338, 476, and 580). However, the activity domains bHLH and PAS are completely identical in the three species.

The *Clock* Similarity Trees. We have used the Kimura distances (30) to generate two trees. One is based on the distances between nucleic acids and the other is based on distances between amino acids (Fig. 2). The method examines each pair of aligned sequences item by item and counts the number of exact matches, partial matches, and gap symbols. If the sequences are nucleic acids, transitions and transversions are also tallied. The *Clock* similarity trees show that *S. judaei*, the youngest species, seems to evolve faster than its older sibling species. Furthermore, *Spalax* is somewhat closer to humans than to mice in CLOCK protein structure (see also Table 1). This result is in contrast with all other phylogenetic trees of *Spalax* derived from other sets of data (6–8).

Function of the Clock/MOP3 Dimer. As already stated above, *Spalax* has a distinctly different polyglutamine (polyQ) repeat (Fig. 1). The *Spalax* MOP3 is very similar to the human MOP3 repeat, but also to the mouse protein. To functionally test whether the difference in the Q-repeat affects *Spalax* Clock activity, we compared *S. galili* Clock with human Clock, which is shorter by 18 aa at the polyQ domain. This was done by an assay that measures transactivation by Clock/MOP3 heterodimer of E-box elements, a type of transcription factor-binding site found adjacent to *Per1* and important for *Per1* expression (25). We found that *Spalax* Clock is a bona fide partner of MOP3 as shown by this E-box/luciferase reporter assay. Note too that its activity is only 30%, hence, it is significantly lower ($P < 0.001$) compared with human protein (Fig. 3). Dimerizing human or *Spalax* Clock with human or *Spalax* MOP3 does not influence their relative activity. However, replacing the Q-rich domain between the two species does invert their relative activity. That is to say, that hClock-sQ as a dimer of either hMOP3 or sMOP3 is as active as sClock, and sClock-hQ as a dimer of either hMOP3 or sMOP3 is as active as hClock (Fig. 3).

The Expression of *Spalax Clock* and *MOP3*. *In situ* hybridization localizes *Spalax Clock* and *MOP3* expression to the SCN in the brain (Fig. 4), the center of the mammalian circadian clock (5). *Spalax Clock* does not oscillate, but its *MOP3* does oscillate, which is similar to what is found in other species studied (23). Furthermore, RT-PCR demonstrates (Fig. 5) that *Spalax Clock* is expressed in several different organs, i.e., in the brain, retina, and harderian gland, as well as in the peripheral tissues kidney and liver. *MOP3* is expressed in all tissues studied. Its expression is quite low in kidney and spleen; however, like *Clock,* it is expressed in those tissues that

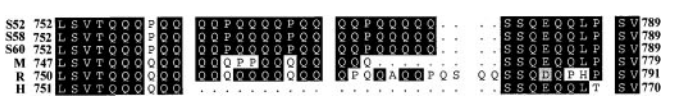

Fig. 1. The Q-rich domain of *Spalax* Clock compared with human, rat, and mouse Clock. *Spalax Clock* was cloned from brain tissues of three species, *Spalax galili* (2*n* = 52), *S. carmeli* (2*n* = 58), and *S. judaei* (2*n* = 60) by RT-PCR, with oligonucleotides from the published sequence of mice, rats, and humans as specified in the text. Two independent clones on both strands confirmed each sequence. The figure depicts a Prettybox of the Clock Q-rich domain of the three *Spalax* species (S52, S58, and S60), humans (H), mice (M), and rats (R). Numbers at both sides represent the amino acids aligned. The figure displaces multiple-sequence alignment in postscript format; shading represents regions that agree with a calculated consensus sequence (Wisconsin package version 10). □, amino acids not similar among the compared species.

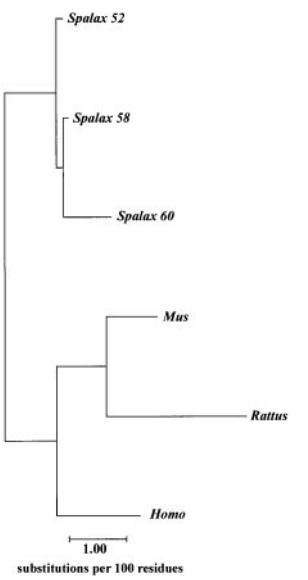

Fig. 2. Similarity tree of the Clock protein. The unrooted tree describes the similarity relationships among the Clock of the three *Spalax* species (S52, S58, and S60), mice (*Mus*), rats (*Rattus*), and humans (*Homo*). The calculated distances show a somewhat closer relationship of *Spalax* Clock to human than to mouse Clock and a faster evolution of the younger *S. judaei* (2*n* = 60) than its older sibling species *S. galili* (2*n* = 52) and *S. carmeli* (2*n* = 58).

EVOLUTION

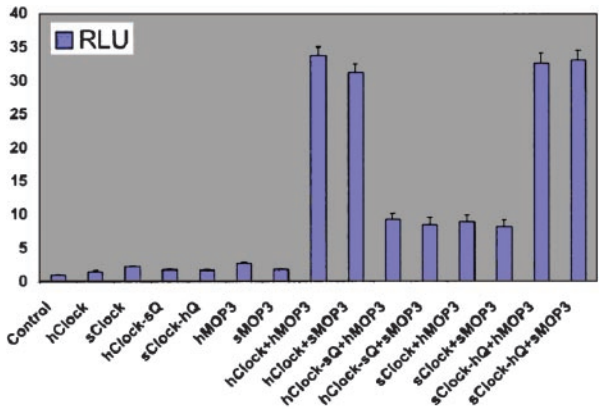

Fig. 3. A comparison of the transcriptional activities of *Spalax* (s) and human (h) *Clock*/*MOP3* dimer. Human hepatoma Hep3b cells were cotransfected with 1 μg of each plasmid expressing the s*Clock* or h*Clock*, s*Clock*-hQ or h*Clock*-sQ, h*MOP3* or s*MOP3*, and the different dimers as specified under the *x* axis of the graph. The M34RE-driven luciferase reporter plasmid (0.2 μg) was also transfected, along with 0.1 μg of the β-galactosidase control plasmid. The luciferase and β-galactosidase activities were measured as described in the text. Relative light units (RLU) were defined as the activity of luciferase divided by that of β-galactosidase (*y* axis). The data represent the mean ± SE of triplicate samples. The difference in activity between the h*Clock* or s*Clock*-hQ with either s*MOP3* or h*MOP3* and the other combinations is highly significant ($P < 0.001$).

are involved in the maintenance of the circadian system, namely brain, eye, and harderian gland. As demonstrated in Fig. 6, *MOP3* also oscillates in the harderian gland, and although its oscillatory pattern is different from its pattern in the SCN, the peak of its expression is identical in both tissues.

Discussion

Circadian rhythm is localized in the central nervous system and is entrained by light signals in the eye. Lightless habitats lead to structural regressive eye evolution (8). Is function also lost? Maintenance of eye rudiments after millions of years in darkness suggests functionality. Blind subterranean mole rats, *S. ehrenbergi* superspecies (Spalacidae, Rodentia) in Israel, have undergone evolutionary tinkering that has optimized molecular and structural reductions and expansions presumably through loss-and-gain of homeotic mutations in organizing a photoperiodic system, adapting to life in total darkness underground (8). In our current work we present data on the cloning, structure, and expression of circadian genes from a visually blind, subterranean mammal.

***Spalax Clock* and *MOP3* Structure.** Despite being a rodent, *Spalax*, an old rodent offshoot (7, 8), is somewhat closer to humans than to mice in *Clock* structure, as was already manifested for some other genes, i.e., *Mhc* loci (33), VEGF cDNA (34), and HMG1 genes (preliminary results). *Spalax* presumably still retains early rodent patterns reorganized and adapted to life underground. *Spalax Clock* demonstrates distinct interspecies polymorphism and *S. judaei,* the youngest species of the *Spalax ehrenbergi* superspecies in Israel (6, 7), seems to evolve faster than the relatively older *S. galili* and *S. carmeli* species, suggesting distinct interspecies divergence across very short geographic distance (≈80 km). This may be due to its unique xeric ecology with large territories and its polyphasic activity pattern in a stressful climate (6–8). Note that already in our first study of activity patterns of different *S. ehrenbergi* species (20), we found that *S. judaei*, which inhabits a significantly warmer and drier environment than the northern species, *S. galili* and *S. carmeli*, has a significantly different activity profile in both levels and patterns. *S. judaei* is less active and has more, albeit shorter, periods of activity, displaying an adaptive strategy of increasing fitness in xeric environments (20).

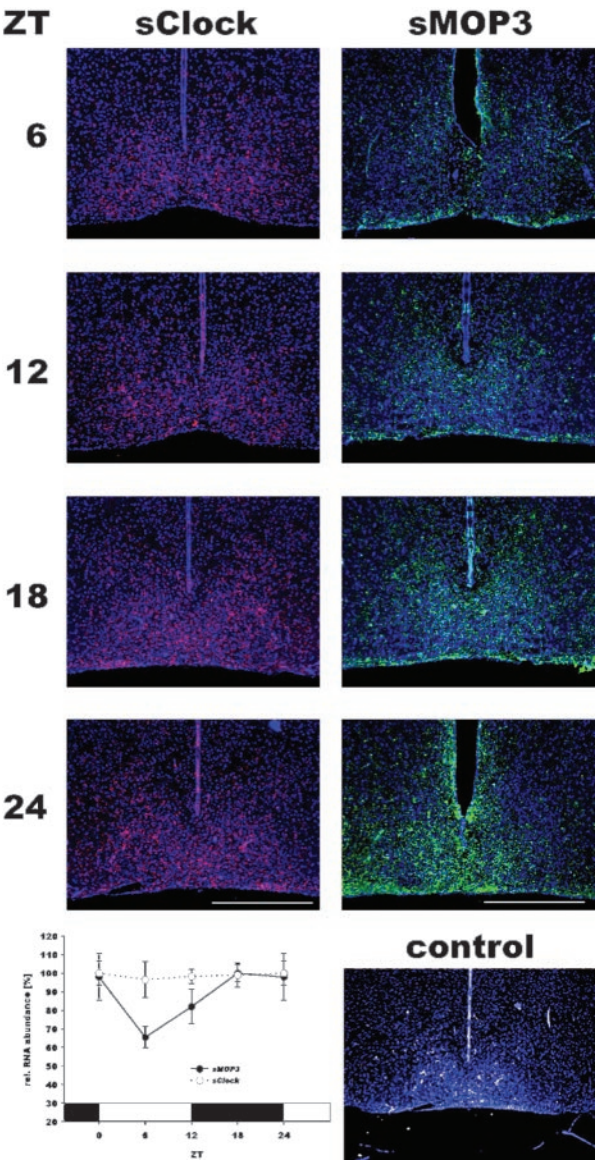

Fig. 4. *In situ* hybridization of *Clock* and *MOP3* in the SCN of *Spalax*. *S. judaei* ($2n = 60$) were killed, and brains were treated as described in *Materials and Methods*. ZT, Zeitgeber time (h). The red grains depict the *Clock*-hybridization areas and the yellow grains depict the *MOP3*-hybridization areas. The control panel (*Bottom Right*) is a negative control carried out with identical, but sense, riboprobes. Notice that, contradictory to *Clock, MOP3* is oscillating as can be seen in the intensity of the colored grains. (Bar = ZT) The graph (*Bottom Left*) is a quantified representation of the *in situ* hybridization. Values are densitometric data done with NIH IMAGE. Maxima are 100% for each gene. Error bars are SD.

Evolution of the *Clock* Gene in *Spalax* Species. The phylogenetic relationship of the four *Spalax* species was analyzed earlier by allozymes (35), mtDNA (36, 37), and DNA–DNA hybridization (38). The tree presented here displaying the interspecies *Clock* similarity relationship of the three *Spalax* species is different from the phylogenetic trees derived from allozymes, mtDNA, and DNA–DNA hybridization. Like the tree derived from cytochrome *b* (39), the *Clock* tree seems to represent not chronological relationships, but a gene tree that describes the rate of ecological evolution of the *Clock* gene in different species. This assumption is supported by the comparison between silent and nonsilent substitutions presented in Table 1. This table shows that the distances with human and mouse *Clock* involves 3 to 7 times more silent substitutions than nonsilent

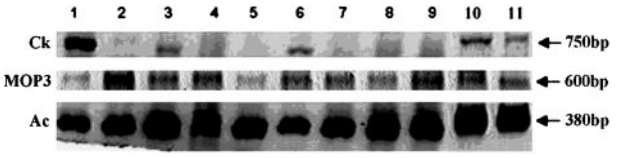

Fig. 5. Tissue distribution of *Clock* and *MOP3* expression in *Spalax*. The distribution of *Clock* (Ck) and *MOP3* expression was characterized by RT-PCR of a fragment of each cDNA, on total RNA samples prepared from the following *S. galili* tissues: kidney (lane 1); intestine (lane 2); liver (lane 3); heart (lane 4); spleen (lane 5); brain (lane 6); muscle (lane 7); testis (lane 8); lung (lane 9); harderian gland (lane 10); and eye (lane 11). The *Clock* gene (*Top*, Ck) is expressed in brain tissue, retina, and harderian gland, as well as in peripheral tissues: kidney and liver. *MOP3* (*Middle*, MOP3) is expressed in all tissues examined, although its relative expression in the kidney (lane 1) and spleen (lane 5) is low. An internal 380-bp fragment of actin cDNA (*Bottom*, Ac) was amplified by RT-PCR in the same reaction tubes as *Clock* or *MOP3*, with actin-specific primers as an internal control.

mutations, which is the usual result when comparing sequences. However, a comparison of the three *Spalax* species exhibits 2 to 3 times more substitutions that cause amino acid changes than those that are synonymous. This is a very unusual observation in phylogenetic trees. The dramatic divergence of the youngest species, *S. judaei*, which displays much faster evolution (more amino acid changes) cannot be reconciled with its relatively recent divergence (6–8, 40). It appears more plausible that *ecological* factors were involved, such as spatiotemporal increasing stressful aridity, which may indirectly affect the circadian pattern, as was demonstrated by radiotracking in time.[§]

Expression and Function of the *Clock*/*MOP3* Dimer. Circadian oscillators appear to be highly conserved throughout evolution and involve transcription-translation negative feedback loops (3, 23). The observation that PAS proteins play an important role in maintaining circadian rhythms supports this idea (41, 42). A distinguishing characteristic of the *Clock* gene is the presence of several functional domains in its amino acid sequence. These are the bHLH (amino acids 34–81), the PAS A direct repeat (amino acids 115–163), the PAS B direct repeat (amino acids 272–318), and the Q-rich domain at the C terminus. Although the bHLH and PAS domains are very conserved among the different *Clock* cDNAs that have been cloned, the most striking difference is in the significant variation in the Q-repeat near the C terminus of Clock. The Q-repeat characterizes the activation domains of many transcription factors (43), and it has been shown to influence circadian rhythmicity (44). It has been shown that A → T nucleotide transversion in a splice donor site, which results in exon skipping and a deletion of 51 aa from the Q-repeat area in the mouse protein, appears to be the cause of a number of changes in the circadian phenotype (45). Most notably, mice homozygous for this deletion manifest a 3–4 h longer period (27–28 h) on initial placement in the dark and then become arrhythmic after a few weeks in darkness. A 6-h exposure to light of these arrhythmic mice restores the long-period rhythmicity. Hence, in addition to a bHLH region (DNA binding domain) and PAS region (protein dimerization domain) Clock also contains a transcriptional activation domain (the Q-rich region). The mutant protein can therefore compete with nonmutant Clock for binding partners and/or DNA binding sites, which explains the dominant negative nature of the mutant allele (44).

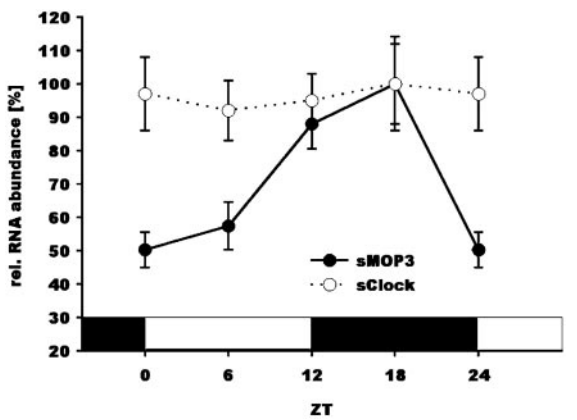

Fig. 6. Expression of *MOP3* and *Clock* in the harderian gland of *Spalax*. *S. galili* ($2n = 52$) kept in a 12-h light/12-h dark cycle were killed at different Zeitgeber time points. Harderian glands were treated as described in *Materials and Methods*. The graph is a quantified representation of the *in situ* hybridization. Values are the densitometric data done with NIH IMAGE. Maxima are 100% for each gene. Notice that contradictory to *Clock, MOP3* is oscillating. Bars are SD.

Evidence demonstrates that proper activity of the circadian system requires heterodimerization of two bHLH-PAS proteins: Clock and MOP3 (25, 26, 46). Our results prove that there is a reduced transcriptional activity ($P < 0.001$) of the *Spalax* Clock/MOP3 dimer compared with humans, possibly increasing metabolic economy (15). The fact that this pattern is retained after interchanging the Q-rich domains of the two species supports an assumption that it is this domain that causes the difference in transcriptional activity. It was already shown that mutant Clock could form heterodimers with MOP3 that bound DNA but failed to activate transcription (46). Moreover, such a mutant, probably by down-regulating the oscillations of *Pers* and *Crys* RNA, leads to reduced levels of *MOP3* transcription, hence limiting the available Clock/MOP3 heterodimers at the appropriate circadian time to drive *Per*/*Cry* transcription and restart the cycle (27). This suggests that Clock, after binding to a specific transcription activation site (the E-box), upstream the initiation site of *Per*, appears to drive the positive component of *Per* transcriptional oscillations, which are thought to underlie circadian rhythmicity. Thus, the *Spalax*-unique Clock may partially inactivate transcription, while retaining the ability to bind DNA and dimerize with partners. Further studies are essential to directly relate the unique polyQ repeat of *Spalax* Clock, with the reduced transactivation by *Spalax* Clock or with its unique polytypic (20), polymorphic (19), and seasonal[§] differences in circadian rhythms. Nevertheless, other differences in the *Spalax Clock* or *MOP3* sequence, although evolutionarily impressive, cannot be related to any presently known functional sites. Hence, the reduced activity of *Spalax* Clock may be cautiously attributed to the different polyQ of its protein. Transgenic mice with *Spalax Clock* may elucidate its direct function.

Tissue Distribution and Oscillation of *Spalax Clock* and *MOP3* Expression. As in other mammals, *Spalax Clock* does not oscillate, but *Spalax MOP3* does oscillate (23). Notably, the oscillatory pattern of *MOP3* in the *Spalax* SCN is a mirror image of that of the mouse *Per1* (32) as well as the *Spalax* equivalent (preliminary results). That is, *MOP3* expression is at its minimum at ZT6, when *Per1* expression is at its maximum. This observation may be explained by Shearman's *et al*. (27) interpretation of the feedback mechanism between Clock/MOP3 heterodimer level and the transcription drive of *Per*/*Cry*.

The tissue distribution of *Spalax Clock* is not restricted to tissues directly related to the maintenance of the biological clock, as was reported in mice (44). It may be involved, as was shown in *Drosophila*, in both circadian (47) and noncircadian oscillations in nonpacemaker tissues (48), or as hypothesized by Yamazaki *et al.* (49) in transgenic rats, that a self-sustained circadian pacemaker in the SCN entrains circadian oscillations in the peripheral tissues. *MOP3* is expressed in all tissues studied, which is similar to what was demonstrated in mice and may reflect its involvement as an orphan dimerizing protein in other transcription activation systems, like the hypoxia-inducible factor (25).

***Clock* and *MOP3* Expression in the Harderian Gland.** We are aware of no other report of expression of circadian genes in the harderian gland. Although the oscillatory pattern of *MOP3* is different from its pattern in the SCN, the peak of its expression is identical in both tissues. This may indicate a unique synchronization of these two tissues that has yet to be clarified, because in other tissues there is always a lag in the peak of expression of oscillatory circadian genes between the SCN and peripheral tissues. The expression of *Clock* and *MOP3* in the harderian gland of *Spalax* is remarkable and should be emphasized: the harderian gland of *Spalax* is tremendously hypertrophied, occupying the entire eye-socket, whereas the eye is degenerated (0.7 mm in diameter), subcutaneous, and embedded in that huge harderian gland. It was previously suggested that the harderian gland of *Spalax* is a possible photoreceptor and photoperiodic organ (11).

Circadian Genes in a Blind Subterranean Mammal. Expression of circadian genes in blind *Spalax* may highlight the genetic basis of its behavioral pattern of circadian rhythmicity (19–22). We have already cloned the *Spalax* cDNA homologs of *Per*1, *Per*2, *Per3*, *Tim, Cry1*, and *Cry*2 (unpublished results). We plan to evaluate their function and their potential convergence in other subterranean mammals. Likewise, the *Spalax* photoreceptor pigment rhodopsin (16) and long-wavelength coneopsin (17, 18, 50) have been cloned and sequenced, and their unique *Spalax* function in photoentrainment was evaluated, presumably as adaptations to life underground by significant enrichment for wavelengths greater than 500 nm, maximizing photon capture, but minimizing the effects of heat (18).

The mosaic evolution of the *Spalax* eye (7, 14, 15), harderian gland (51), and brain (52), and its circadian genes provides a dramatic model of tinkering evolution at both the molecular and organismal levels. From an evolutionary perspective, the genetic basis of circadian rhythms in blind subterranean mole rats may be different from that of strictly diurnal or nocturnal and sighted mammals. The identification of the blind *Spalax Clock* might help, together with its other circadian genes, highlighting the structure and evolution of the circadian organization in mammals, including humans, at the molecular level and their ecological causation. Furthermore, it may highlight both adaptive evolution linking structure and function and behavioral–molecular interactions of regression, progression, and convergence in subterranean mammals generally, and especially in the Pleistocene ecological speciation of the *Spalax ehrenbergi* superspecies caused by increasing ecological aridity stresses (6–8), which in turn affect the patterns of circadian rhythmicity. It could also elucidate, by transgenic studies in mice, the control of the *Spalax*-unique polyphasic, polymorphic, and seasonal cycles, as well as sleeping disorders, work shifts, and jetlag in humans.

We thank Dr. J. Takahashi for the mouse *Clock* probe and Dr. C. Bradfield for his experimental help and advice with the transcriptional activation assay. We are also grateful to Mr. Michael Margulis for his help with the computer graphic work. This work was supported by a grant from Human Frontier Science Program and by the Ancell–Teicher Research Foundation for Genetics and Molecular Evolution.

1. Feldman, J. F. (1982) *Annu. Rev. Plant Physiol.* **33,** 583–608.
2. Edmunds, L. N., Jr. (1988) *Cellular and Molecular Bases of Biological Clocks: Models and Mechanisms for Circadian Timekeeping* (Springer, New York).
3. King, D. P. & Takahashi, J. S. (2000) *Annu. Rev. Neurosci.* **23,** 713–742.
4. Wager-Smith, K. & Kay, S. A. (2000) *Nature (London)* **26,** 23–27.
5. Ralph, M. R., Foster, R. G., David, F. C. & Menaker, M. (1990) *Science* **247,** 975–978.
6. Nevo, E., Ivanitskaya, E. & Beiles, A. (2001) *Adaptive Radiation of Blind Subterranean Mole Rats* (Backhuys, Leiden, The Netherlands)
7. Nevo, E. (1991) *Evol. Biol.* **25,** 1–125.
8. Nevo, E. (1999) *Mosaic Evolution of Subterranean Mammals: Regression, Progression, and Global Convergence* (Oxford Univ. Press, Oxford).
9. Nevo, E. (1998) in *Principles of Animal Design: The Optimization and Symmorphosis Debate*, eds. Weibel, E. R., Taylor, C. R. & Bolis, C. (Cambridge Univ. Press, Cambridge, U.K.), pp. 288–298.
10. Haim, A., Heth, G., Pratt, H. & Nevo, E. (1983) *J. Exp. Biol.* **107,** 59–64.
11. Pevet, P., Heth, G., Haim, A. & Nevo, E. (1984) *J. Exp. Zool.* **232,** 41–50.
12. Rado, R., Gev, H., Goldman, B. D. & Terkel, J. (1991) in *Photobiology*, ed. Riklis, E. (Plenum Press, New York), pp. 323–331.
13. Sanyal, S., Jansen, H. G., de Grip, W. G., Nevo, E. & de Jong, W. W. (1990) *Invest. Ophthalmol. Visual Sci.* **31,** 1398–1404.
14. Cooper, H. M., Herbin, M. & Nevo, E. (1993) *Nature (London)* **361,** 156–159.
15. Cooper, H. M., Herbin, M. & Nevo, E. (1993) *J. Comp. Neurol.* **328,** 313–350.
16. Janssen, J. W. H., Bovee-Geurts, P. H. M., Peeters, Z. P. A., Bowmaker, J. K., Cooper, H. M., David-Gray, Z. K., Nevo, E. & DeGrip, W. J. (2000) *J. Biol. Chem.* **275,** 38674–38679.
17. David-Gray, Z. K., Janssen, J. W. H., Nevo, E & Foster, R. G. (1998) *Nat. Neurosci.* **12,** 655–656.
18. David-Gray, Z. K., Cooper, H. M., Jenssen, J. W. H., Nevo, E. & Foster, R. G. (1999) *FEBS Lett.* **461,** 343–347.
19. Ben-Shlomo, R., Ritte, U. & Nevo, E. (1995) *Behav. Genet.* **25,** 239–245.
20. Nevo, E., Guttman, R., Haber, M. & Erez, E. (1982) *J. Mammal* **63,** 453–463.
21. Tobler, I., Nevo, E. & Hermann, M. (1998) *Behav. Brain Res.* **96,** 173–183.
22. Goldman, B. D., Goldman, S. L., Riccio, A. P. & Terkel, J. (1997) *J. Biol. Rhythms* **12,** 348–361.
23. Dunlap, J. C. (1999) *Cell* **96,** 271–290.
24. Kyriacou, C. P. (1990) *Behav. Genet.* **20,** 191–211.
25. Hogenesch, J. B., Gu., Y. Z., Jain, S. & Bradfield, C. A. (1998) *Proc. Natl. Acad. Sci. USA* **95,** 5474–5479.
26. Bunger, M. K., Wilsbacher L. D., Moran, S. M., Clendenin, C., Radcliffe, L. A., Hogenesch, J. B., Simon, M. C., Takahashi, J. S. & Bradfield, C. A. (2000) *Cell* **103,** 1009–1017.
27. Shearman, L. P., Sriram, S., Weaver, D. R., Maywood, E. S., Chaves, I., Zheng, B., Kume, K., Lee, C. C., van der Horst, G. T., Hastings, M. H. & Reppert, S. M. (2000) *Science* **288,** 1013–1019.
28. Veres, G., Gibbs, R. A., Scherer, S. E. & Caskey, C. T. (1987) *Science* **237,** 415–417.
29. Kimura, M. (1983) *The Neutral Theory of Molecular Evolution* (Cambridge Univ. Press, Cambridge, U.K.).
30. Weir, B. S. (1996) in *Genetic Data Analysis II* (Sinauer Associates, Sunderland, MA), p. 356.
31. Albrecht, U., Sun, Z., Eichele, G. & Lee, C. (1997) *Cell* **91,** 1055–1064.
32. Abe, H., Honma, S., Namihira, M., Takahasi, Y., Ikeda, M., Yu, W. & Honma, K. (1999) *Brain Res. Mol. Brain. Res.* **20,** 104–110.
33. Schopfer, R., Figueroa, F., Nizetic, D., Nevo, E. & Klein, J. (1987) *Mol. Biol. Evol.* **4,** 287–299.
34. Avivi, A., Resnick, M. B., Nevo, E., Joel, A. & Levy, A. P. (1999) *FEBS Lett.* **452,** 133–140.
35. Nevo, E., Filippucci, M. G. & Beiles, A. (1994) *Heredity* **72,** 465–487.
36. Nevo, E., Honeycutt, R. L., Yonekawa, H., Nelson, K. & Hanzawa, N. (1993) *Mol. Biol. Evol.* **10,** 590–604.
37. Nevo, E. & Beiles, A. (1992) *Biol. J. Linn. Soc.* **47,** 385–405.
38. Catzeflis, F. M., Nevo, E., Ahlquist, J. E. & Sibley, C. G. (1989) *J. Mol. Evol.* **29,** 223–232.
39. Nevo, E., Beiles, A. & Spradling, T. (1999) *J. Mol. Evol.* **49,** 215–226.
40. Nevo, E., Tchernov, E. & Beiles, A. (1988) *Z. Zool. Syst. Evol. Forsch.* **26,** 286–314.
41. Kay, S. A. (1997) *Science* **276,** 753–754.
42. Gu, Y. Z., Hogenesch, J. & Bradfield, C. (2000) *Annu. Rev. Pharmacol. Toxicol.* **40,** 519–561
43. Mitchell, P. J. & Tjian, R. (1989) *Science* **245,** 371–378.
44. Antoch, M. P., Song, E. J., Chang, A. M., Vitaterna, M. H., Zhao, Y., Wilsbacher, L. D., Sangoram, A. M., King, D. P., Pinto, L. H. & Takahashi, J. S. (1997) *Cell* **89,** 656–667.
45. King, D. P., Zhao, Y., Sangoram, A. M., Wilsbacher, L. D., Tanaka, M., Antoch, M. P., Steeves, T. D., Vitaterna, M. H., Kornhauser, J. M., Lowrey, P. L., *et al.* (1997) *Cell* **89,** 641–653.
46. Gekakis, N., Stakins, D., Nguyen, H. B., Davis, H. B., Wilsbacher, L. D., King, D. P., Takahashi, J. S. & Weitz, C. J. (1998) *Science* **280,** 1564–1569.
47. Darlington, T. K., Wager-Smith, K., Ceriani, M. F., Staqnis, D., Gekakis, N., Steeves, T. D. L., Weitz, C. J., Takahashi, J. S. & Kay, S. A. (1998) *Science* **280,** 1599–1603.
48. Kyriacou, C. P. & Hall, J. C. (1980) *Proc. Natl. Acad. Sci. USA* **77,** 6929–6933.
49. Yamazaki, S., Numano, R., Abe, M., Hida, A., Takahashi, R. Ueda, M., Block, G. D., Sakaki, Y., Menaker, M. & Tei, H. (2000) *Science* **288,** 682–685.
50. Argamaso, S. M., Froehlich, A. C., McCall, M. A., Nevo, E., Provencio, I. & Foster, R. G. (1995) *Biophys. Chem.* **56,** 3–11.
51. Balemans, M. G. M., Pevet, P., Legerstee, W. C. & Nevo, E. (1980) *J. Neural Transm.* **49,** 247–255.
52. Rehkamper, G., Necker, R. & Nevo, E. (1994) *J. Comp. Neurol.* **347,** 570–584.